Experimental Evaluation of a Fiber Optics Gyroscope for Improving Dead-reckoning Accuracy in Mobile Robots

Johann Borenstein

Dept. of Mech. Eng., The University of Michigan
Ann Arbor, MI 48109

ABSTRACT

This paper presents results from the experimental evaluation of a state-of-the-art fiber-optics gyroscope. The purpose of our experiments was to evaluate the suitability of this gyroscope for enhancing dead-reckoning in mobile robots. The evaluated gyroscope was the "*Autogyro Navigator*" made by Andrews. For a 4×4 m square path the dead-reckoning error when using this gyro was less than ±1.2° in orientation and about 10 cm (4 in) in position.

1. INTRODUCTION

One of the foremost problems in mobile robotics is the determination of the robot's momentary location and orientation (collectively called "positioning"). While there are many different methods for positioning [Borenstein et al., 1996], almost all mobile robots use at least one method, called "dead-reckoning." Dead-reckoning is the collective term for all those positioning methods that do not use external beacons or other references. The most widely used form of dead reckoning is odometry – positioning based on counting wheel revolutions. Other possible components of a dead-reckoning system are accelerometers and gyroscopes.

Figure 1: The Andrew *Autogyro Navigator* fiber-optics gyroscope. (Courtesy of [Andrew].)

Gyroscopes measure rotational rate, which can be integrated to yield changes in orientation. It is widely understood that the foremost problem with gyros is their inherent "*bias-drift*" (also referred to as "*drift rate*" or "*drift*"), which, after integration, results in unbounded growth of the desired orientation measurement. A thorough treatment of all types of gyroscopes is given in [Everett, 1995], while a good theoretical and experimental evaluation of two low-cost gyroscopes is provided in [Barshan and Durrant-Whyte, 1995].

A relatively new type of gyroscopes, called, fiber-optics gyro, has recently become available for a cost of about $1K, which makes them attractive for mobile robot applications. The drift-rate of these fiber-optics gyros is as low as that of high-quality conventional mechanical gyros costing fifty times as much. Because of their low drift rate fiber-optics gyro allow several minutes of motion before a new bias-drift measurement must be made. In Section 2 we discuss methods for measuring bias drift with gyroscopes and we present some results. Komoriya and Oyama [1994] tested a fiber optics gyroscope made by [HITACHI] on a mobile robot and provide some experimental results for that gyro.

In our experiments we used another commercially available fiber-optics gyroscope, the *Autogyro Navigator* (or, as we will call it in short: *Navigator*), which is made by Andrew Corp. [ANDREW]. This device cost $900 in early 1997[1]. This *Navigator*, shown in Figure 1, is especially designed for land-based navigation. It is a single-axis interferometric fiber-optic gyroscope based on polarization-maintaining fiber and precision fiber-optic gyroscope technology [Borenstein et al., 1996]. Table I provides the basic technical specifications, while a more in-depth discussion of the technology used in the *Navigator* is given in [Allen et al., 1994; Bennett and Emge, 1994].

One less appreciated problem with fiber-optics gyros is the non-linearity of their *scale factor* (SF). The SF is a fixed value that is specified by the manufacturer and that tells the user how to convert the gyro's output values to degrees-per-second. Section 3 addresses these issues in more detail. Experimental results from using the *Navigator* on a mobile robot are presented in Section 4.

---

[1] Shortly before this paper went to press we learned that Andrew Corp. sold its gyro division to KVH Industries [KVH]. KVH now markets the Autogyro Navigator under the name E-Core RA/RD 2000 and the price is US$1,950.

Table I: Technical specifications for the Andrew *Autogyro Navigator*

Parameter	Value	Units
Input rotation rate	± 100	°/s
Instantaneous band-width	100	Hz
Bias drift at stabilized temperature — RMS	0.005	°/s rms
	18	°/hr rms
Size (excluding connector)	115×90×41	mm
	4.5×3.5×1.6	in
Weight (total)	0.25	Kg
	0.55	lb
Power Analog	< 2	W
Power Digital	< 3	W

2. STATIC BIAS CALIBRATION

The first and easiest-to-measure performance criterion of a gyro is its static readout as a function of time. Figure 2 shows a plot of rate measurements for the *Navigator,* while the gyro is stationary. One obvious interpretation of the test results in Figure 2 is that the bias drift is related to sensor temperature.

It is possible to build a look-up table based on the apparent relation between drift rate and sensor temperature shown in Figure 2. Doing so may provide a notable improvement in many applications. For this reason, the *Navigator* comes equipped with a built-in temperature sensor that can be read during operation. However, we found that even with a bias drift look-up table the resulting bias-drift estimate is not as accurate as that obtained from the static bias test, described next.

In many mobile robot applications there are stages in which the mobile platform is stationary before moving on to a new location. Under these conditions it is feasible that the system performs a *static bias test*. In this test gyro readings are taken for, say, 20 seconds, every time the mobile robot is known to be stationary. The average of these readings, denoted ω_{bias}, is from then on subtracted from subsequent readings during travel. We have found that this method provides generally better results than determining ω_{bias} from a temperature-based look-up table – provided the gyro is operating under steady state conditions and provided the subsequent travel takes only a few minutes until the next static bias test is performed.

3. SCALE FACTOR CALIBRATION

As mentioned before, the linearity of the *scale factor* (SF) is an often-overlooked component of overall accuracy.
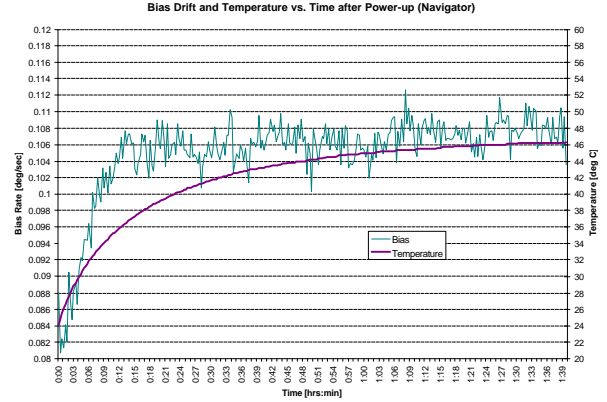

Figure 2: Bias drift and temperature versus time after power-up.

The SF is a number provided by the manufacturer, which converts the output of the gyroscope (typically a voltage or a dimensionless number) to degrees per second (°/s). A perfectly linear SF would provide an accurate conversion that is exactly proportional to the rate of rotation at all operating rates of rotation. In practice, however, the SF varies slightly, depending on temperature, rate of rotation, direction of rotation, and possibly other factors.

In order to measure the SF of the *Navigator* we constructed a test-bed based on an inexpensive stepper motor-driven rotary table from [ARRICK]. We also developed software that allowed precise control of this rotary table – a non-trivial task that required the development of accurate timing routines to implement precision step-intervals and precise acceleration and deceleration.

In a typical test we would mount the gyro at the center of the table and rotate the table through 360° first in clockwise (cw), then in counter-clockwise (ccw) direction, at a fixed speed. At the beginning and end of each turn the table would be accelerated and decelerate as fast as possible without losing steps. Throughout this paper we will refer to such a precisely defined 360° rotation as a cw- or ccw-*turn.* We will use the term *run* to refer to a sequence of one turn in cw direction, immediately followed by one turn in ccw direction.

During each turn the gyro readings were integrated to yield the measured change of orientation, θ_{meas}. At the end of each 360° turn, we computed the error

$$E_{cw} = -\theta_{meas,\ cw} - 360° \qquad (1a)$$

for the turn in cw direction (θ_{meas} was always negative in ccw turns), and

$$E_{ccw} = +\theta_{meas,\ ccw} - 360° \qquad (1b)$$

for the turn in ccw direction (θ_{meas} was always positive in ccw turns)

Once the error E for a particular set of parameters (e.g., temperature or rate of rotation) is know, it is possi-

ble to correct subsequent rate readings by defining one or more correction factors. Furthermore, based on the actually measured θ_{meas} we can define correction factors

$$C_{cw} = 360°/|\theta_{meas, cw}| = 360°/|E_{cw} + 360°| \qquad (2a)$$

and

$$C_{ccw} = 360°/|\theta_{meas, ccw}| = 360°/|E_{ccw} + 360°| \qquad (2b)$$

which can be applied to subsequent rate readings as

$$\omega^* = \omega_{raw} \times SF \times C_{cw/ccw} \qquad (3)$$

where ω_{raw} is the raw gyro reading (a dimensionless number) and ω^* is the scaled and corrected rate in units of degrees-per-second (°/s).

If several different correction factors have been identified, then Eq. 3 can be extended

$$\omega^* = \omega_{raw} \times SF \times C_{1, cw/ccw} \quad \times C_{2, cw/ccw} \times \ldots$$
$$\ldots \times C_{n, cw/ccw} \qquad (4)$$

Using this experimental setup and the notation of Eq. 1 we measured the performance of the gyro against changes in different parameters, and we defined correction factors, as discussed next.

Our first concern was the expected non-linearity of the SF as a function of temperature. Since temperature information is part of the output stream of the *Navigator*, it is a straightforward matter to build a look-up table that provides a scale-factor correction value for different temperatures.

To do so, the rotary table was programmed to perform many runs, as follows: Immediately before *each* run a *static bias test* of 20 seconds duration was performed, to determine the current bias drift. The thus measured bias drift was subtracted from all gyro readings in the subsequent run. Then the run (i.e., one 360° rotation in cw and one 360° rotation in ccw direction) was performed at a fixed steady state speed of 30°/s. At the end of each run the errors E_{cw} and E_{ccw} (see Eq. 1) were recorded and plotted against the temperature of the gyro during that run. Starting to record this data shortly after power-up and continuing until the gyro reached steady state temperature assured that a wide range of temperatures was covered. Steady state temperature was usually reached after about two hours. Each run and its associated *static bias test* took about 48 seconds.

Results for the temperature calibration of the *Navigator* are shown in Figure 3. Compared to our experience with an earlier model fiber-optics gyro the results for the *Navigator* turned out to be unexpectedly accurate, as evident from Figure 3. Because of the highly linear relation between temperature and scale factor we fitted a linear trend line to the data using the equation

$$E_{T, cw/ccw} = -0.52 \times T + 19.23 \qquad (5)$$
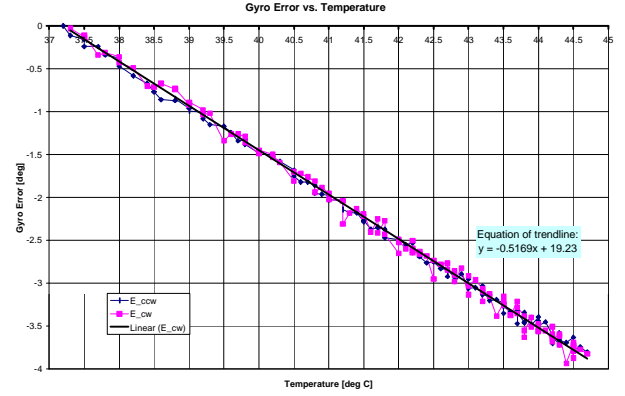
where T is the measured temperature in °C.

Figure 3: Errors resulting from scale factor non-linearity in the rotary table experiment with the *Navigator* gyro were found to be linearly proportional to the internal temperature of the gyro.

Note that data sets for both E_{cw} and E_{ccw} are plotted in Figure 3 and that both data sets are equally well described by Eq. 5. We can thus assume $E_{T,cw} \approx E_{T,ccw}$ for the *Navigator*. Using the notation of Eq. 2 and substituting Eq. 5, a temperature correction factor was defined:

$$C_{T, cw/ccw} = 360°/|E_{T,cw/ccw} + 360°| =$$
$$360°/(379.23 - 0.52 \times T) \quad (6)$$

Our experiments showed that using Eq. 6 to compensate for the effect of sensor temperature on the *Navigator's* SF was very effective and provided accurate compensation.

It should be noted that when we discussed our results with the manufacturer of the *Navigator*, [ANDREW], the Andrew engineers explained that SF temperature compensation similar to Eq. 6 was already applied by the processor inside the *Navigator*. Each *Navigator*, we were told, was calibrated at the factory so that the end user would not have to perform the calibration that led to our Figure **3**. In other words, the data sets of Figure 3 should closely resemble a horizontal straight line. The Andrew engineers suggested that the calibration at the factory might have gone wrong *for our particular unit.* However, even though Andrew offered a free re-calibration of our unit at their site, we chose to continue working with our unit using Eq. 6 for calibration.

In order to evaluate the benefits of our SF correction with regard to temperature (i.e., Eq. 6) we performed numerous tests on the rotary table. In each test run the momentary static bias was determined over a period of 20 seconds, followed by a single run (i.e., a full cw and ccw turn). The results are shown in Fig. 6 for the *Navigator* after temperature correction. Note that each run was completely independent, there is thus no meaning to the lines connecting the data points. Nonetheless, we chose to plot

the connecting lines to make it easier to identify all cw and all ccw results.

To summarize the results of Fig. 6: For a full 360°-turn in either cw or ccw direction the error in the amount of rotation as measured by the gyro was typically less than ±0.2° and less than ±0.25° in all cases.

4. EXPERIMENTAL RESULTS ONBOARD A MOBILE ROBOT

All of the experiments described in this section were performed on the University of Michigan's Cybermotion K2A mobile robot called "CARMEL" (see Figure 4). Our first series of experiments, described in Section 4.1, aimed at measuring the accuracy of the gyro without attempting to use the gyro readings to improve the dead-reckoning accuracy of the robot. A second set of experiments, described in Section 4.2, aimed at using the gyro readings to improve the dead-reckoning accuracy of the robot. The difference between these two aims is far from trivial.

Figure 4: The University of Michigan's mobile robot CARMEL (based on a Cybermotion K2A).

4.1 Experimental measurement of gyro performance only

In all of the experiments CARMEL was programmed to move along a 4×4 m square path with a total rotation of 360° in both cw and ccw direction. At the end of each cw or ccw lap a precise absolute position and orient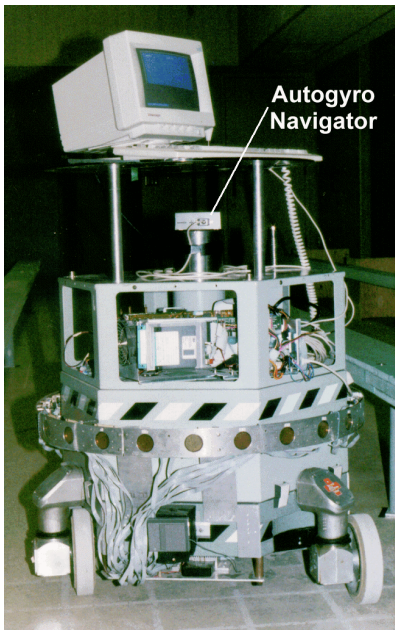ation measurement was taken to compare the actual total rotation of the robot to the rotation derived from the gyro readings. We estimate the accuracy of the absolute measurement to be ±2 mm in position and ±0.2° in orientation. The result of each mobile robot test was thus an error that expressed the difference between the actual amount of rotation and the amount of rotation measured by the gyro. We will refer to this error as the "*return orientation error*" E_g.

In the beginning of each lap a 20-seconds *static bias test* (see Section 2) was performed. Then an initial absolute position measurement was taken and the robot ran through the lap. At the end of each lap another absolute position measurement was taken and compared to the orientation derived from the gyro's measurements. The maximum speed during straight-line segments was 0.4 m/s and the maximum speed during the four 90° turns was 30°/s. The total travel time for each lap was 64 seconds.

Results from a 16-hour test with 40 runs (each run comprising one cw and one ccw lap) with the *Navigator* mounted on CARMEL are shown in Figure 5. For comparison we have included the *return orientation errors* resulting from odometry only (the lines labeled E_{odo_cw} and E_{odo_ccw} in Figure 5. Note that these errors (averaging -2° and -6° for the cw and ccw laps, respectively) are much larger than what one could reasonably expect from the Cybermotion K2A platform using odometry only. We attribute these large errors to the poor mechanical shape our 10-year old CARMEL is in. Nonetheless, the return orientation errors based on the gyro readings are contained within ±1°.
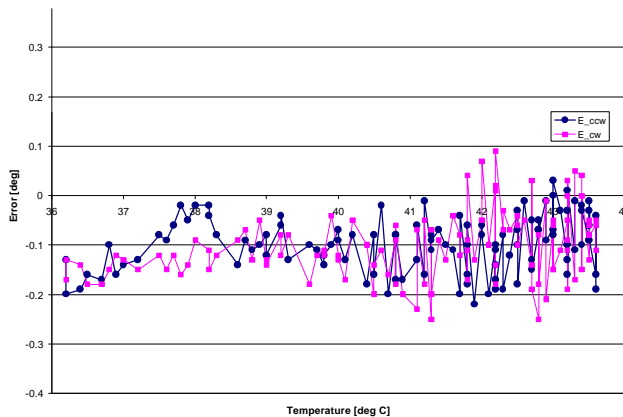

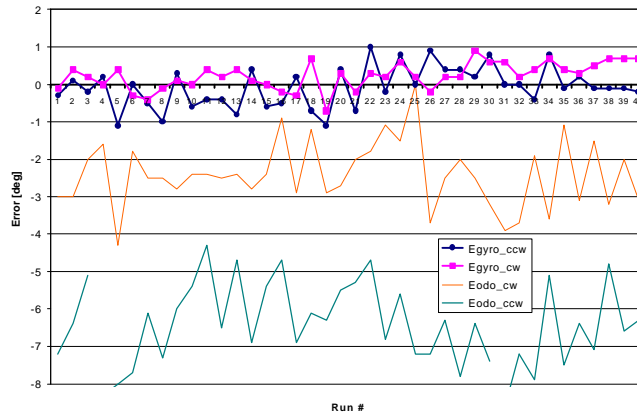**Figure 6:** Turn errors after SF temperature compensation, based on Eq. 6.

Figure 5: Experimental results from using the Autogyro Navigator onboard CARMEL.

4.2 Experimental evaluation of gyro-enhanced dead-reckoning

This section explains how the data from the *Navigator* was used to correct the K2A-platform's built-in odometry system. This task is non-trivial because of some peculiarities in the K2A's user interface. Specifically, the K2A's odometry system is inaccessible for the user during motion. For this reason it is impossible to correct the K2A's heading variable with more accurate gyro-derived heading data while the platform moves. The K2A heading variable can only be corrected when the platform is stationary. Consequently the robot may follow an erroneous trajectory based on its inaccurate odometry. For example, we found that in a 10 m straight-line motion segment a heading error of over 1° may accumulate as the robot actually follows a slightly curved trajectory (likely due to unequal wheel diameters and misalignment of wheels). As we noted before, this unexpectedly large error is likely due to the poor mechanical condition of CARMEL.

To overcome the problem of not being able to send odometry updates to the onboard controller we implemented multiple controllers during straight line and turning motion. These controllers are described next.

4.2.1 Gyro-enhanced straight-line motion

For straight-line motion we designed three different control loops:

1. The desired linear velocity is prescribed by our control program and maintained by the K2A built-in controller. We achieve acceleration and deceleration by ramping up or down the prescribed speed.
2. When approaching the end-point of the prescribed straight-line segment, a position control loop is invoked that modifies the prescribed linear speed to allow accurate stopping within ±2 mm of the desired end-point.
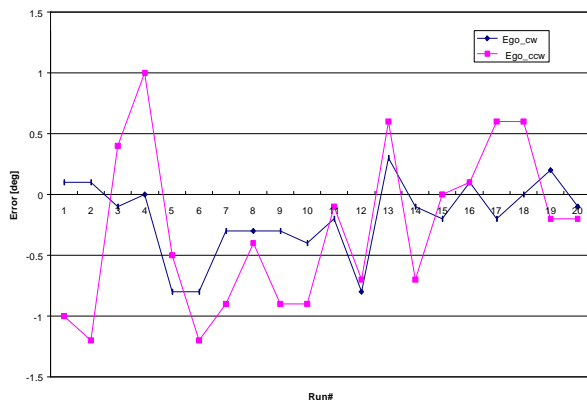
3. A steering correction control loop, closed by gyro data, produces small steering corrections designed to maintain the true heading of the robot constant. This is a counter-intuitive procedure for a synchro-drive platform like the K2A, because straight-line motion is ideally implemented by simply powering the drive motor and leaving the steering motor unpowered. Nonetheless, the overlaid steering control works well and maintains platform heading within ±0.3°.

After completing each straight-line motion segment the position of the robot is computed based on the linear displacement measured by the K2A odometry system and the final orientation measured by the gyro. The thus gyro-corrected position/orientation is downloaded to the K2A built-in odometry system for use in subsequent motion.

4.2.2 Gyro-enhanced on-the-spot turning

In on-the-spot turning motion two different control loops are used:

1. The desired rotary velocity is prescribed by our control program and maintained by the K2A built-in controller. We achieve acceleration and deceleration by ramping up or down the prescribed rotary speed.
2. When approaching the final heading of the prescribed pure rotary motion segment, an orientation control loop is invoked that modifies the prescribed rotary speed to allow accurate stopping within ±0.1° of the desired endpoint. The orientation control loop is closed through the gyro, not the K2A's odometry system.

4.2.3 Results from gyro-enhanced odometry

Experimental results of the system described above are shown in Figs. 7 and 8. Figure 7 shows the *return orientation errors* after completing the bi-directional square
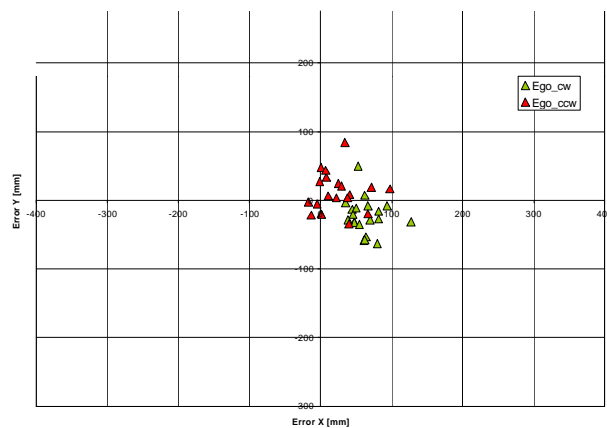

Figure 7: Return *orientation* errors after completing the bi-directional square path. K2A odometry was corrected with gyro data after each motion segment.

Figure 8: Return *position* errors after completing the bi-directional square path. K2A odometry was corrected with gyro data after each motion segment.

path. Figure 8 shows the associated *return position errors* for the same 20 consecutive runs.

The return orientation errors are within ±1.2°, slightly larger the ±1.0°-measurement error of the gyro seen in Figure 5. The reason for this discrepancy is the K2A's internal odometry computation, which works with a resolution of 0.3°. Consequently any odometry result obtained from the internal K2A odometry system (such as the results in Figure 7) will have an additional error of up to 0.3° due to the limited resolution.

All but one return position error fall into a square of 10×10 cm (4×4 in). For comparison we have included Figure 9, which shows the return position errors of our K2A platform in the same experiment, but *without* gyro corrections. We should emphasize, however, that these very poor odometry-only results are mostly due to the poor mechanical condition of our K2A platform.

5. CONCLUSIONS

In this paper we presented results from three groups of experiments with the *Autogyro Navigator* fiber-optics gyroscope made by [ANDREW]. The experiments were performed with the gyro mounted on a) a rotary table, for base line tests, and on a mobile robot, for "real-world" tests. In the third group of experiments the gyro data was used to correct odometry errors on the mobile robot and the overall dead-reckoning accuracy of the robot was evaluated.

The rotary table experiment showed that the *Navigator's* measurement error for 360°-turns was consistently within ±0.25° under ideal laboratory conditions. When mounted on a mobile robot the gyro errors after traveling through a 4×4 m square path (with a total of 4×90° = 360° turning) were within ±1.0°. When the gyro data was used
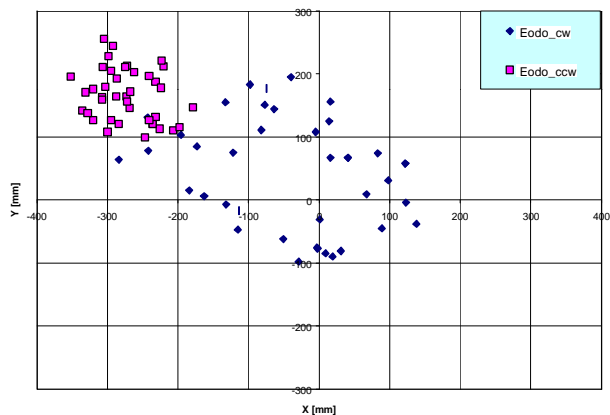

Figure 9: Return position errors after completing the bi-directional square path experiment *without* gyro correction (i.e., no use of gyro at all).

to correct the robot's odometry the odometry errors were within ±1.2° in orientation and within roughly ±10 cm in position.

The accuracy produced in our tests with the *Navigator* (±1° for a 360° square path) compares favorably to the rotational accuracy obtained from odometry on most other mobile platforms (see [Borenstein and Feng, 1994] for comparison data from other platforms).

6. REFERENCES

Allen, D. et al., 1994, "A Low Cost Fiber Optic Gyro for Land Navigation." Presented at the SPIE Annual Meeting, San Diego, CA, July.)

Barshan, B. and Durrant-Whyte, H.F., 1995, "Inertial Navigation Systems Mobile Robots." *IEEE Transactions on Robotics and Automation*, Vol. 11, No. 3, June 1995, pp. 328-342.

Bennett, S. and Emge, S.R., 1994, "Fiber Optic Rate Gyro for Land Navigation and Platform Stabilization." Presented at Sensors Expo '94, Cleveland, OH, Sept. 20.

Borenstein, J. and Evans, J., 1997, "The OmniMate Mobile Robot – Design, Implementation, and Experimental Results." *Proceedings of the 1997 IEEE International Conference on Robotics and Automation*, Albuquerque, NM, Apr. 21-27, 1997, pp. 3505-3510.

Borenstein, J., Everett, B., and Feng, L., 1996, "*Navigating Mobile Robots: Systems and Techniques.*" A. K. Peters, Ltd., Wellesley, MA, ISBN 1-56881-058-X.

Borenstein, J. and Feng. L., 1995b, "UMBmark: A Benchmark Test for Measuring Dead-reckoning Errors in Mobile Robots." *Presented at the 1995 SPIE Conference on Mobile Robots*, Philadelphia, PA, October, 1995.

Everett, H.R. 1995, "*Sensors for Mobile Robots.*" A K Peters, Ltd., Wellesley, MA.

Komoriya, K. and Oyama, E., 1994, "Position Estimation of a mobile Robot Using Optical Fiber Gyroscope (OFG)." *International Conference on Intelligent Robots and Systems* (IROS '94). Munich, Germany, September 12-16, pp. 143-149.

ANDREW – Andrew Corporation, 10500 W. 153rd Street, Orland Park, IL 60462. Ph.: 708-349-5294.

ARRICK – Arrick Robotics, P.O. Box 1574, Hurst, TX, 76053. Ph: 817-571-4528.

HITACHI - Hitachi Cable America, Inc., New York Office, 50 Main Street, 12th floor, White Plains, NY 10606, Ph.: 914-993-0990.

KVH – KVH Industries, Inc. KVH Industries, Inc. Middletown, RI 02842, Ph.: 401-847-3327